OPEN ACCESS Freely available online

PLoS one

A Computational Analysis Framework for Molecular Cell Dynamics: Case-Study of Exocytosis

Wenhai Chen[1,2☯], Wen Zhou[3☯], Tian Xia[4,5*], Xun Gu[1,6*]

1 School of Life Sciences and Center for Evolutionary Biology, Fudan University, Shanghai, China, **2** College of Mathematics & Information Science, Wenzhou University, Zhejiang, China, **3** Department of Mathematics, Iowa State University, Ames, Iowa, United States of America, **4** Electrical and Computer Engineering Department, Iowa State University, Ames, Iowa, United States of America, **5** Biomedical Informatics Center, Northwestern University Clinical and Translational Sciences Institute, Chicago, Illinois, United States of America, **6** Department of Genetics, Development, and Cell Biology, Iowa State University, Ames, Iowa, United States of America

Abstract

One difficulty in conducting biologically meaningful dynamic analysis at the systems biology level is that *in vivo* system regulation is complex. Meanwhile, many kinetic rates are unknown, making global system analysis intractable in practice. In this article, we demonstrate a computational pipeline to help solve this problem, using the exocytotic process as an example. Exocytosis is an essential process in all eukaryotic cells that allows communication in cells through vesicles that contain a wide range of intracellular molecules. During this process a set of proteins called SNAREs acts as an engine in this vesicle-membrane fusion, by forming four-helical bundle complex between (membrane) target-specific and vesicle-specific SNAREs. As expected, the regulatory network for exocytosis is very complex. Based on the current understanding of the protein-protein interaction network related to exocytosis, we mathematically formulated the whole system, by the ordinary differential equations (ODE). We then applied a mathematical approach (called inverse problem) to estimating the kinetic parameters in the fundamental subsystem (without regulation) from limited *in vitro* experimental data, which fit well with the reports by the conventional assay. These estimates allowed us to conduct an efficient stability analysis under a specified parameter space for the exocytotic process with or without regulation. Finally, we discuss the potential of this approach to explain experimental observations and to make testable hypotheses for further experimentation.

Citation: Chen W, Zhou W, Xia T, Gu X (2012) A Computational Analysis Framework for Molecular Cell Dynamics: Case-Study of Exocytosis. PLoS ONE 7(7): e38699. doi:10.1371/journal.pone.0038699

Editor: Huaijun Zhou ,University of California, Davis, United States of America

Received February 1, 2012; **Accepted** May 14, 2012; **Published** July 11, 2012

Funding: The authors have no support or funding to report.

Competing Interests: The authors have declared that no competing interests exist.

* E-mail: xgu@iastate.edu (XG); tianxia@northwestern.edu (TX)

☯ These authors contributed equally to this work.

Introduction

Exocytosis is the fundamental physiological process that leads the traffic of vesicles to fuse with the plasma membrane, releasing its vesicle contents into targeted cells that control many cellular processes [1–3]. Substantial studies have shown that it involves multiple steps from vesicle trafficking, docking, priming to fusion [1–14]. During this process, a set of proteins called SNARE proteins occupy a central position in the fusion by protein-protein interacting between vesicular-specific and (membrane) target-specific SNARE protein isoforms, denoted by vSNARE and tSNARE, respectively. Moreover, this SNARE-mediated fusion is highly regulated through different modes [6,15–23]. For instance, one mode is through the protein-protein interaction with MUNC18, a member of Sec1/Munc18 (SM) protein family, while the other mode is through the Ca^{2+}-triggered exocytosis [14,15,5,20].

Although experimental studies have provided invaluable insights for the underlying exocytosis mechanisms, the process of exocytosis is a typical example to show the difficulty in conducting an analysis at the systems biology level [24–28]. That is, while the biochemical reaction chain is straightforward and simple, the regulation *in vivo* of the system is complex. As many kinetic rates are unknown, and concentrations of proteins, complexes and substrates keep changing in both *vivo* and *vitro* environments, a biologically meaningful, global system analysis is intractable in practice. Earlier, Mezer et al. [10] proposed a computational platform to model the exocytotic process. They formulated these protein interactions into a sequential (feed-forward only without any regulation) interaction pathway to describe the exocytotic system dynamics.

In this paper, we utilize the exocytotic process as a model system to present a computational framework for system modeling and analysis. Similar to [10], we model the dynamics and architecture of the complex system by the ordinary differential equations (ODEs). First, we model the whole system by taking the regulatory elements into account. Second, we use a math techniques called inverse problem to estimate the rate parameters for the basic steps of biochemical reactions. Through the method, we are able to recover and optimize these parameters based on limited *in vitro* experimental data. Third, based on the above estimates, we can therefore approximately study the stability behavior of this system with and without MUNC18 regulation. We then attempt to explain experimental observations about different fusion efficiency caused by the change of SNARE proteins' concentration and multiple complexes in the SNARE-induced membrane fusion. Moreover, we make a few interesting predictions that can be verified by further experimentations.

Results and Discussion

The Protein Interaction Network of Exocytosis

From the view of gene network, the exocytotic process is a sophisticated combination of sequential interactions of well-defined proteins and protein complexes [1–13]. As shown in Fig.1, it has three major components. The first step of the basic reaction component includes two membrane proteins, SNAP25 (synaptosome-associated protein, 25 kDa) and syntaxin, together forming the so-called tSNARE; here t means target, the plasma membrane where the vesicle is heading for. Another important protein is vesical-associated membrane protein (VAMP2), belonging to the category of vSNARE (vesicle). In the second step, the protein complex formed by tSNARE and vSNARE is the fundamental step for the membrane fusion. In our study we consider two regulatory components, which are MUNC18-mediated and Ca^{2+}-dependent regulation pathways, respectively. On the other hand, from the view of systems biology the mechanism of this exocytotic process is a dynamics system capturing the temporal change of the concentrations of proteins and intermediate complexes, which can be formulated based on an ODE dynamic system, as shown below in details.

The basic steps. The well-known foundations [4,3,8] for this exocytotic processes are the following two reactions.

$$SNAP25 + syntaxin \overset{k_1/k_{-1}}{\rightleftharpoons} tSNARE$$

$$tSNARE + VAMP2 \overset{k_2/k_{-2}}{\rightleftharpoons} FHC$$

where the protein complex FHC stands for the four-helical bundle. Formation of FHC complex is the main step to promote membrane fusion, an essential part of exocytosis. In addition, there are several follow-up complex modifications. For instance, the function of complexin is as a clamp [20], resulting in

$$FHC + complexin \overset{k_3/k_{-3}}{\rightleftharpoons} FC$$

where FC is the generic notation for the protein complex of FHC and complexin.

Ca^{2+}-dependent regulation. Ca^{2+} is the main trigger for the initiation of intracellular exocytosis [4,14,15,5]. Suggested by [16,4], the regulation of Ca^{2+} is executed through stimulating synaptotagmin. A well-known mechanism is that Ca^{2+} binds with the SNARE complexes (FHC) and stimulates the fusion [2]. The reaction equations to characterize the mechanism regarding Ca^{2+} and synaptotagmin are given by

$$synaptotagmin + Ca^{2+} \overset{k_{-4}/k_{-4}}{\rightleftharpoons} CaS$$

where CaS stands for the complex of synaptotagmin and one Ca^{2+} ion, and

$$CaS + 3Ca^{2+} + FC \overset{k_{-5}/k_{-5}}{\rightleftharpoons} FHC^{*} + complexin$$

$$CaS + 3Ca^{2+} + tSNARE \overset{k_{-6}/k_{-6}}{\rightleftharpoons} Tsc$$

$$CaS + 3Ca^{2+} + FHC \overset{k_{-7}/k_{-7}}{\rightleftharpoons} FHC^{*}$$

where the generic notation Tsc represents the protein complex of tSNARE and synaptotagmin binding four Ca^{2+} ions, and FHC^{*} represents the complex of FHC and synaptotagmin binding four Ca^{2+} ions.

MUNC18-dependent regulation. MUNC18 is an important regulatory protein for the exocytotic system [6,17,22], through two different modes: (*i*) MUCNC18 associates with syntaxin to remove them from the assembly into the SNARE complexe at the beginning stage; and (*ii*) MUNC18 stimulates the fusion process by associating with FHC. These two reaction mechanisms can be written as follows.

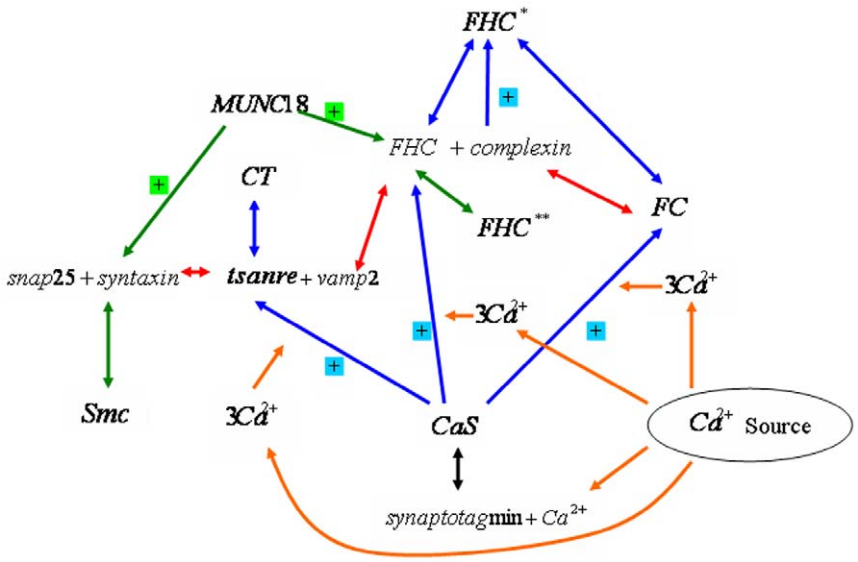

Figure 1. The whole process of fusion used in the mathematical model is shown. One direction arrows and symbol of "+" represent the reaction between proteins, ions and complexes, while full direction arrows connect two parts of a single reaction. Modified from [1–6].
doi:10.1371/journal.pone.0038699.g001

$$MUNC18 + FHC \overset{k_8/k_{-8}}{\rightleftharpoons} FHC^{**}$$

where FHC** is the complex of MUNC18 and FHC to help the fusion process; and

$$MUNC18 + syntaxin \overset{k_0/k_{-0}}{\rightleftharpoons} Smc$$

where Smc is the generic name for the protein complex of MUNC18 and syntaxin.

Mathematical Modeling for the Whole Exocytotic System

Putting together, we have formulated a mathematical model by the ordinary differential equations (ODE) to capture how the concentrations of different proteins and complexes vary with time and how they interact each other. Based on the law of mass action and Michaelis-Menten Kinetics, and using the conventional notation $[\cdot]$ for the concentration, the ODE system is given by.

$$\frac{d[SNAP25]}{dt} = -k_1[SNAP25][syntaxin] + k_{-1}[tSNARE]$$

$$\frac{d[syntaxin]}{dt} = -k_1[SNAP25][syntaxin] + k_{-0}[Smc]$$

$$-k_0[syntaxin][MUNC18] + k_{-1}[tSNARE]$$

$$\frac{d[VAMP2]}{dt} = -k_2[tSNARE][VAMP2] + k_{-2}[FHC]$$

$$\frac{d[synaptotagmin]}{dt} = -k_4[synaptotagmin][Ca^{2+}] + k_{-4}[CaS]$$

$$\frac{d[complexin]}{dt} = -k_3[FHC][complexin] + k_5[CaS][FC][Ca^{2+}]^3$$

$$-k_{-5}[FHC^*][complexin] + k_{-3}[FC]$$

$$\frac{d[MUNC18]}{dt} = -k_0[MUNC18][syntaxin] + k_{-0}[Smc]$$

$$+k_{-8}[FHC^{**}] - k_8[MUNC18][FHC]$$

$$\frac{d[FC]}{dt} = k_3[FHC][complexin] + k_{-5}[FHC^*][complexin]$$

$$-k_{-3}[FC] - k_5[CaS][FC][Ca^{2+}]^3$$

$$\frac{d[CT]}{dt} = k_6[CaS][tSNARE][Ca^{2+}]^3 - k_{-6}[CT]$$

$$\frac{d[CaS]}{dt} = k_{-6}[CT] + k_{-7}[FHC^*] - k_7[CaS][FHC][Ca^{2+}]^3$$

$$+k_{-5}[FHC^*][complexin]$$

$$-k_5[CaS][FC][Ca^{2+}]^3 - k_6[CaS][tSNARE][Ca^{2+}]^3$$

$$-k_{-4}[CaS] + k_4[synaptotagmin][Ca^{2+}]$$

$$\frac{d[Smc]}{dt} = k_0[MUNC18][syntaxin] - k_{-0}[Smc]$$

$$\frac{d[tSNARE]}{dt} = k_1[SNAP25][sytaxin] + k_{-2}[FHC] + k_{-6}[CT]$$

$$-k_{-1}[tSNARE]$$

$$-k_2[tSNARE][VAMP2] - k_6[CaS][tSNARE][Ca^{2+}]^3$$

$$\frac{d[FHC]}{dt} = k_2[tSNARE][VAMP2] + k_{-3}[FC] + k_{-8}[FHC^{**}]$$

$$+k_{-7}[FHC^*] - k_{-2}[FHC] - k_3[FHC][complexin]$$

$$-k_8[MUNC18][FHC] - k_7[CaS][FHC][Ca^{2+}]^3$$

$$\frac{d[FHC^*]}{dt} = k_5[CaS][FC][Ca^{2+}]^3 + k_7[CaS][FHC][Ca^{2+}]^3$$

$$-k_{-5}[FHC^*][complexin] - k_{-7}[FHC^*]$$

$$\frac{d[FHC^{**}]}{dt} = k_8[MUNC18][FHC] - k_{-8}[FHC^{**}] \qquad (1)$$

One may raise the question, due to the complexity of this network, whether we have empirical evidence enough to show the concept we try to put forward. In a recent article, we [29] have conducted a comparative network motif analysis for the Sec1/

Munc18-SNARE regulatory mechanisms through a comprehensive compile of experimental data from different species and different cell types. In spite of some differences in details that have been shown important for cell-specific and species-specific system behaviors, we confidently conclude that Eq.(1) may conceptually represent the basic dynamic system that is likely universal. Some comments about Eq.(1) are presented below.

Dynamics of Ca^{2+}. The dynamics for Ca^{2+} in exocytosis is complex. To be analytically feasible, we assume that during the fusion process, concentration of Ca^{2+} ions at active zone is temporal dependent. Thus, the dynamics of Ca^{2+} ions around the region of fusion (active zone) can be characterized as.

$$\frac{d[Ca^{2+}]}{dt} = k_{-6}[CT] + k_{-7}[FHC^*] + k_{-5}[FHC^*][complexin]$$

$$-k_5[CaS][FC][Ca^{2+}]^3 - k_4[synaptotagmin][Ca^{2+}]$$

$$-k_6[CaS][tSNARE][Ca^{2+}]^3 + k_{-4}[CaS]$$

$$-k_7[CaS][FHC][Ca^{2+}]^3 + S(Ca^{2+}) \quad (2)$$

where $S(Ca^{2+})$ is the recruitment source of calcium. Nevertheless, the *in vivo* concentration of Ca^{2+} ions may stay at a roughly constant level as both external and internal sources may have kept the balance of Ca^{2+}. In this case, Eq.(2) can be replaced by the simplest form $Ca^{2+} = \text{Constant}$.

Self-association of syntaxin. We notice that self-association of syntaxin is possible such that $i \underset{\epsilon_{-i}}{\overset{\epsilon_i}{\rightleftharpoons}} syntaxin_i$, where $i = 5,6,7,8$, syntaxin^i represents the complexes made of i syntaxins [12]. Hence, if we take the effect of self-association into account, the system of Eq.(1) needs to be modified as follows: we have the equation for the concentration of syntaxin.

$$\frac{d[syntaxin]}{dt} = -k_1[SNAP25][syntaxin] + k_{-0}[Smc]$$

$$+k_{-1}[tSNARE] - k_0[syntaxin][MUNC18]$$

$$-\sum_{i=5}^{8} \epsilon_i [syntaxin]^i + \sum_{i=5}^{8} \epsilon_{-i}[syntaxin_i] \quad (3)$$

and additional four equations to describe the dynamics of self-associated complexes, that is,

$$\frac{d[syntaxin_i]}{dt} = \epsilon_i [syntaxin]^i - \epsilon_{-i}[syntaxin_i] \quad (4)$$

where $i = 5,6,7,8$

Mass conservation. One can show that the ODE system of Eq.(1) complies with the detailed balance principle and the mass conservation. For instance, because the only products of the reactions involving MUNC18 are Smc and FHC**, the change of concentration of MUNC18 is only relevant to the concentrations of these two complexes. Indeed, for the subsystem that only involves MUNC18, Smc and FHC**, we obtain.

$$\frac{d}{dt}([Smc] + [MUNC18] + [FHC^{**}]) = 0$$

$$\Rightarrow [MUNC18](t) = [MUNC18](0) - [Smc](t) - [FHC^{**}](t) \quad (5)$$

since there are no Smc and FHC** initially.

Spatial effect. Denote all of the variables (concentrations) in Eqs.(1)–(5) by a vector U so that the ODE system can be rewritten in a concise form of $dU/dt = f(U)$, where f is vector of functions on the right hand side of each equation. If the spatial effects of proteins and protein complexes are considered, this system should be generally written as follows.

$$\frac{dU}{dt} = f(U) + D_U \cdot \Delta U \quad (6)$$

where D_U stands for the vector of diffusion coefficients of proteins, complexes and ions. Study of reaction diffusion equations described by Eq.(6) would be interesting particularly for the problems related to the developmental process.

Estimation of Reaction Rate Parameters

The whole system for the exocytotic process as described in Eq.(1) is a typical example to show the general difficulty in systems biology [24–28]. While the biochemical reaction chain is simple, the regulation *in vivo* of the system can be very complex. In addition, most paremeters remain unknown in this ODE system, including the initial concentrations of different proteins and complexes, and the reaction rates in both *vivo* and *vitro* environments. Hence, it is almost intractable in practice to carry out a global system analysis. As a first step to overcome this difficulty, we attempt to estimate the rate parameters for the basic steps of exocytotic process. Among different methods, we choose the technique of inverse problem that has two advantages: the required data size is small, and the algorithm guarantees the uniqueness and efficiency [25].

The fundamental subsystems. As the well-known machinery, chemical reactions.

$$SNAP25 + syntaxin \overset{k_1/k_{-1}}{\rightleftharpoons} tSNARE + VAMP2 \overset{k_2/k_2}{\rightleftharpoons} FHC$$

are fundamental for membrane fusion. The behavior of this subsystem involving only proteins SNAP25, syntaxin and VAMP2 can be described as

$$\frac{d[SNAP25]}{dt} = -k_1[SNAP25][syntaxin] + k_{-1}[tSNARE]$$

$$\frac{d[syntaxin]}{dt} = -k_1[SNAP25][syntaxin] + k_{-1}[tSNARE]$$

$$\frac{d[VAMP2]}{dt} = -k_2[tSNARE][VAMP2] + k_{-2}[FHC]$$

$$\frac{d[tSNARE]}{dt} = k_1[SNAP25][sytaxin] + k_{-2}[FHC]$$

$$-k_{-1}[tSNARE]-k_2[tSNARE][VAMP2]$$

$$\frac{d[FHC]}{dt}=k_2[tSNARE][VAMP2]-k_{-2}[FHC] \qquad (7)$$

Using the inverse problem technique [30] to estimate rate parameters requires initial concentrations. In the following the symbol $[u](0)$ is used for the concentration of variable u at time $t=0$. From the experimental data [9], we set the initial condition for system Eq.(10) to be: $[SNAP25](0)=[Syntaxin](0)=9[VAMP2](0)=9\mu m/L$, and $[tSNARE](0)=[FHC](0)=0$. It should be noticed that the estimation of kinetic rate parameters are usually insensitive to the initial conditions, as verified by our simulation studies (not shown).

Reparameterization for data-fitting. In the experimentation, researches use the fluorescence intensity, $x(t)$ to measure the time-dependent fusion process. The relationship between the concentrations of core complexes (FHC, FHC*, FHC**) and the fluorescence intensity, $x(t)=C([FHC],[FHC^*],[FHC^{**}])$, needs to be addressed in some details. Some experimental studies such as [11] suggested that the function C can be roughly considered to be linear when the signal strength is far below the saturated level. In this case we have.

$$x(t)=c_1\cdot[FHC^*]+c_2\cdot[FHC^{**}]+c_3\cdot[FHC] \qquad (8)$$

where $c_i,(i=1,2,3)$ are unknown constants. We further assume that the generated intensity of fluorescence due to fusion is $x_g(t)=[FHC](t)$ and the measured intensity of fluorescence is $x(t)=x_g(t)+x_0(t)$, where $x_0(t)$ is a constant supply for fluorescence, resulting in

$$\frac{dx}{dt}=\frac{dx_g}{dt}=c\cdot\frac{d[FHC]}{dt}. \qquad (9)$$

Employing Eqs.(8)-(9) in the system Eq.(7), denote $[SNAP25]=u_1$, $[Syntaxin]=u_2$, $[VAMP2]=u_3$, $[tSNARE]=v_1$, $[FHC]=v_2$ (or $(x(t)=c\cdot v_2(t))$, we have

$$\frac{du_1}{dt}=-k_1u_1u_2+k_{-1}v_1$$

$$\frac{du_2}{dt}=-k_1u_1u_2+k_{-1}v_1$$

$$\frac{du_3}{dt}=-k_2v_1u_3+k_c{}'x$$

$$\frac{dv_1}{dt}=k_1u_1u_2+k_{c'}x-k_{-1}v_1-k_2u_3v_1$$

$$\frac{dx}{dt}=k_cv_1u_3-k_{-2}x \qquad (10)$$

where $k_c=k_2$ and $k_{c'}=k_{-2}/c$. Thus, parameter recovery for the fundamental subsystem equivalent to identify the parameters $(k_{\pm1},k_{\pm2},c)$ of Eq.(10).

Estimation by the inverse problem algorithm. To recover the appropriate reaction rates, we apply technique introduced by [27] to Eq.(10). Some useful theorems are presented in the section of Materials and Methods. Using the data from [9], the identified parameters are shown in the table 1. We compare the numerical results based on the identified parameters with experimental data in Fig.2, and the error is $\sim10^{-4}$.

Stability Analysis of the Fundamental Subsystem

Estimation of rate parameters of the subsystem Eq.(10), as summarized in Table 1, allows us to carry out the stabilizing analysis under a specified parameter space. Considering the subsystem Eq.(10) with v_2 instead of $x(t)$, we first study the fundamental subsystem without any regulation, under the initial concentrations $u_1(0)$, $u_2(0)$, $u_3(0)$, $v_1(0)$ and $v_2(0)$ for proteins SNAP25, Syntaxin, and VAMP2, and protein complexes tSNARE and FHC, respectively. While the formal mathematical treatment is shown in the section of Data and Methods, below we discuss about the biological interpretations.

Our analysis has shown that the final steady state level of the fusion is highly dependent on initial concentrations. Obviously, three proteins (SNAP25, syntaxin and VAMP2) must exist at $t=0$ so that $u_1(0)>0$, $u_2(0)>0$ and $u_3(0)>0$. It is reasonable to assume no any fusion (here measured by FHC) at the initial time point, which means $v_2(0)=0$. The only case we have to deal with carefully is the initial concentration of tSNARE complex, $v_2(0)$. This is because in *vivo*, tSNARE is already preformed in the plasmic membrane; and then carried by vesicles, vSNARE (VAMP2 in our case) binds with it to generate fusion. In this sense, we assume $v_1(0)\geq0$ in general.

To be concise, we define $c_1=u_1(0)-u_2(0)$, $c_2=u_3(0)+v_2(0)$, and $c_3=u_1(0)+v_1(0)+v_2(0)$ and $K=k_{-1}/k_1$. Let $\bar{u}_i$ $(i=1,2,3)$ and $\bar{v}_i$ $(i=1,2)$ be the steady-states for $[SNAP25]$, $[Syntaxin]$, $[VAMP2]$, $[tSNARE]$ and $[FHC]$, respectively, and the steadt state vector $P=(\bar{u}_1,\bar{u}_2,\bar{u}_3,\bar{v}_1,\bar{v}_2)$. Our goal is to obtain the analytical form of P. As shown in the section of Data and Methods, our mathematical analysis considers three cases under the specified parameter space given by Table 1.

(*A*) Case-A assumes that the initial concentration of SNAP25 and syntaxin are the same such that $c_1=0$. Denote $K=k_{-1}/k_1$, provided $k_{-2}<<k_2$, we have shown there are two locally stable-steady states, denoted by P_1 and P_2, respectively, corresponding to $c_2>c_3$ or $c_2<c_3$. If $c_2=c_3$, the degenerated steady state P is also stable.

(*B*) Case-B studies the problem without the assumption of same initial concentration of SNAP25 and syntaxin. Our stability analysis shows that, provided $k_{-i}<<k_i$ where $i=1,2$, there are four steady states of P that are locally stable, corresponding to (*i*) $c_1\leq0$ and $c_3\geq c_2$, (*ii*) $c_1\leq0$ and $c_3\leq c_2$, (*iii*) $c_1\geq0$ and $c_3\geq c_2+c_1$, and (*iv*) if $c_1\geq0$, $c_3\leq c_2+c_1$, and $c_3\geq c_1$, respectively.

(*C*) Case-C considers a more general case that the reaction ratio k_{-1}/k_1 and concentrations of SNARE proteins and complexes are in the same order, that is, $K:=k_{-1}/k_1\in(10^{-8}M,10^{-6}M)$ and $K':=k_{-2}/k_2\tilde{1}0^{-10}M$. It has been shown taht the steady-states are locally stables under the following conditions: (*i*) $c_1\leq0$ and $c_3\leq c_2$; (*ii*) $c_1\geq0$, $c_3\leq c_2+c_1$ and $c_3\geq c_1$; and (*iii*) $c_3\geq c_2$ and $c_3\geq c_2+c_1$, respectively.

Since we are mostly interested in the final steady state-level of fusion, i.e., $\bar{v}_2=[FHC]$, the biological meaning of above stability analyses can be summarized in Table 2. In short, for the system

Table 1. Reaction rates for the fundamental subsystem.

Reaction rates	Estimated interval (95%)	From references
k_1	$4.40\times10^{3}M^{-1}s^{-1}\sim2.30\times10^{6}M^{-1}s^{-1}$	$6.0\times10^{3}M^{-1}s^{-1}$, [18]
k_{-1}	$3.76\times10^{-6}s^{-1}\sim0.549\times10^{-2}s^{-1}$	$1.0\times10^{-2}s^{-1}$, [21]
k_2	$3.60\times10^{4}M^{-1}s^{-1}\sim3.10\times10^{6}M^{-1}s^{-1}$	$1.0\times10^{5}M^{-1}s^{-1}$, [19]
k_{-2}	$1.96\times10^{-4}s^{-1}\sim1.69\times10^{-3}s^{-1}$	$4.2\times10^{-4}s^{-1}$, [23]
c	$1.24\ cd/(M/L)\sim6.20\ cd/(M/L)$	Not available

Note: k_1 is the reaction rate for $SNAP25+syntaxin\rightarrow tSNARE$; k_{-1} is for $SNAP25+syntaxin\leftarrow tSNARE$; k_2 is for $tSNARE+VAMP2\rightarrow FHC$, k_{-2} is for $tSNARE+VAMP2\leftarrow FHC$, and c is the fusion-concentration constant.
doi:10.1371/journal.pone.0038699.t001

involving SNAP25, Syntaxin and VAMP2, we should only consider two types of initial conditions: If the initial conditions only include initial concentrations of SNAP25, Syntaxin and VAMP2, but no tSNARE, the final steady state of fusion $[FHC]$ is equal to the least initial concentration of SNAP25, Syntaxin and VAMP2. In the case of non-zero initial concentration of tSNARE ($[tSNARE]_0>0$), however, the final steady state $[FHC]$ can be much higher as long as the initial concentration of VAMP2 (vSNARE) is sufficiently large. This case is particularly interested because in *vivo*, SNAP25 and Syntaxins may have been already preincubation (preformed) into tSNAREs on the plasmic membrane, before vSNARE proteins (VAMP2 in our case) approach, as carried by vesicles.

Our analysis explains why the outcome of fusion process depends on the way to put these three proteins into the system [21]. One is the sequential process: SNAP25, Syntaxin and VAMP2 proteins are added into the system in order such that virtually no tSNARE protein complex has been formed when the reaction begins. The other one is the preformed process: After SNAP25 and Syntaxin proteins have been preincubation (preformed) into tSNARE, VAMP2 proteins are then added to initiate the fusion reaction. Numerical simulations have shown that the preformed process reaches the steady state much faster than the sequential one (Fig.3), which is consistent with *in vitro* experimental data (the embedded panel) [21].

Stability Analysis on MUNC18-dependent Regulation

We furthermore study the stability behavior of the system involving the regulatory protein MUNC18. As discussed above,

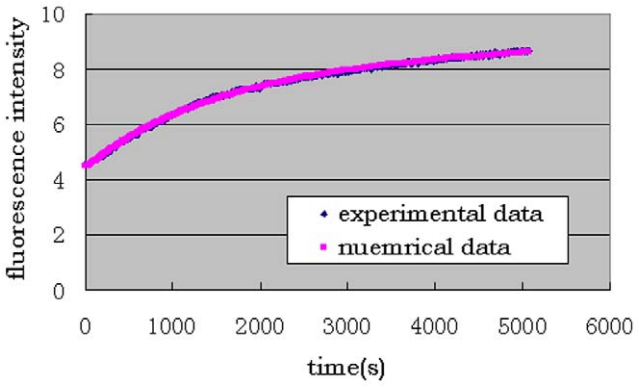

Figure 2. A comparison to the good-of-fit level between the numerical results by the inverse problem analysis and the original experimental data from [9]. The error is about 10^{-4}.
doi:10.1371/journal.pone.0038699.g002

the MUNC18-dependent regulation has two types: (*i*) It binds tightly to a closed conformation of sytanxin that precludes the syntaxin's involvement in the fusion process, suggesting that MUNC18 inhibits fusion by regulating the formation of tSNARE. And (*ii*) it can assemble with SNARE complexes (FHC) to accelerate membrane fusion in late stages when the concentration of four helical bundles (FHC) is high enough.

We make the following assumptions to simplify the subsystem with MUNC18-dependent regulation. Considering the situation that tSNARE has been preformed and reaction of SNAP25, sytanxin and tSNARE has reached the equilibrium, we claim that the function of MUNC18 can be characterized as follows.

$$tSNARE+VAMP2\overset{k_2/k_{-2}}{\rightleftharpoons}MUNC18+FHC\overset{k_8/k_{-8}}{\rightleftharpoons}FHC^{**}$$

where FHC** is the complex of MUNC18 and FHC, and it behaves similar to FHC to help the fusion process; and

$$tSNARE+MUNC18\overset{p}{\rightarrow}\{SNARE-MUNC18\}$$

where p stands for the binding rate of MUNC18 onto the syntaxin in closed conformation. In the above reactions, the concentrations of four helical bundles, FHC, and four helical bundles binding with MUNC18, FHC** reflect the level of fusion. It has been shown that the disassociation rate of MUNC18-syntaxin complex is very small comparing to the binding rate, so that the second reaction is considered as an irreversible one.

Introducing variables $[vSNARE]=u_3$, $[tSNARE]=v_1$, $[FHC]=v_2$, $[MUNC18]=u_4$, and $[FHC**]=v_3$, the subsystem involving MUNC18 is rewritten as.

$$\frac{dv_2}{dt}=k_3u_3v_1+k_{-4}v_3-k_4v_2v_4-k_{-3}v_2$$

$$\frac{du_3}{dt}=-k_2v_1u_3+k_{-3}v_2$$

$$\frac{dv_3}{dt}=-k_{-4}v_3+k_4v_2u_4$$

$$\frac{dv_1}{dt}=k_3u_3v_1+k_{-3}v-2-pu_4v_1$$

Table 2. A brief summary for the stabilizing analysis of the fundamental subsystems without regulation.

Initial condition for the first reaction	Initial condition for the second reaction	Fusion level at steady state, [FHC]
$[SNP25]_0 \le [Syntaxin]_0$	$[VMP2]_0 > [SNAP25]_0 + [tSNARE]_0$	$[FHC] = [SNAP25]_0 + [tSNARE]_0$
$[SNP25]_0 \le [Syntaxin]_0$	$[VMP2]_0 < [SNAP25]_0 + [tSNARE]_0$	$[FHC] = [VMP2]_0$
$[SNP25]_0 > [Syntaxin]_0$	$[VMP2]_0 < [Syntaxin]_0 + [tSNARE]_0$	$[FHC] = [VMP2]_0$
$[SNP25]_0 > [Syntaxin]_0$	$[VMP2]_0 > [Syntaxin]_0 + [tSNARE]_0$	$[FHC] = [Syntaxin]_0 + [tSNARE]_0$

doi:10.1371/journal.pone.0038699.t002

$$\frac{du_4}{dt} = k_{-4}v_3 - k_4 v_2 u_4 - p u_4 v_1 \tag{11}$$

Using the mathematical approaches similar to the case of no regulation, we have studied the stability of system Eq.(11). Assume the binding rate p, reaction rates $k_{\pm 4}$ are in the range given by the reference [17–19], we have shown the existence of steady states of Eq.(11), including bi-stability. As the result has been rigorously presented in the section of Data and Methods, we are mainly interested in the final fusion level, as measured by $F = FHC + FHC^{**}$. Under the assumption that the initial concentration of FHC** is zero, i.e., $v_3(0) = 0$, we interpret our results as follows.

(*i*) If $[MUNC18]_0 - [FHC]_0 \le [tSNARE]_0 \le [VAMP2]_0 + [MUNC18]_0$, there exist two bi-stable states for the final fusion levels: One is the high fusion level, which is given by.

$$F_{high} = [VAMP2]_0 + [tSNARE]_0 \tag{12}$$

In this case, at the steady state, the concentrations of free MUNC18 and free vSNARE (VAMP2) are virtually zero, which mean all of these proteins exist in the form of FHC and/or FHC**. The second steady-state is the low fusion level (F_{low}), the

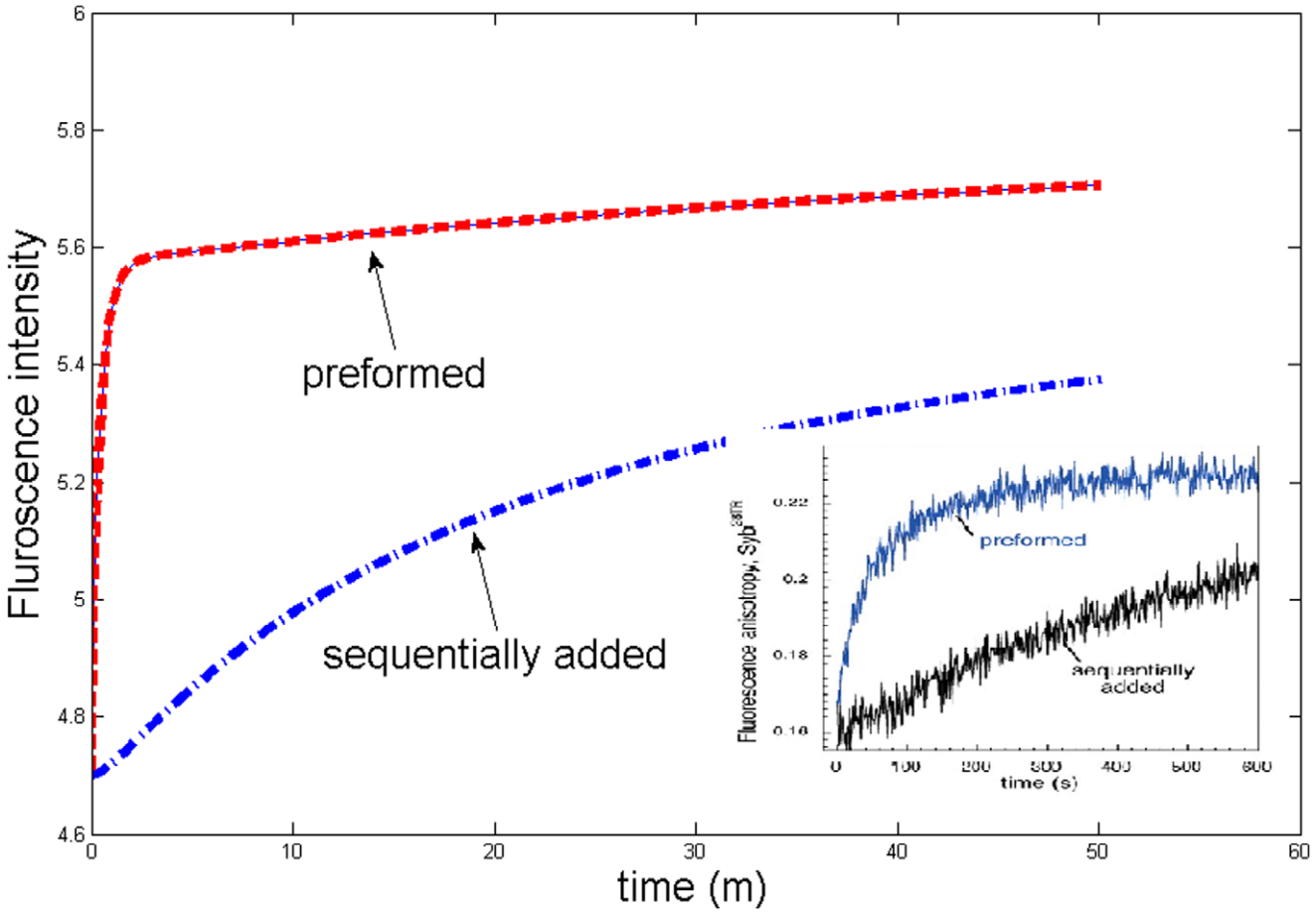

Figure 3. A comparison between proformed and sequential fusion processes. Numerical simulation results are presented, whereas the experimental results are in the embedded plot from [21].
doi:10.1371/journal.pone.0038699.g003

up-bound of F_{low} is actually $F_{low}^{+}=F_{high}$, whereas the low-bound is given by.

$$F_{low}^{-}=2[tSNARE]_0-[MUNC18]_0 \tag{13}$$

On the other hand, the low steady state fusion level, F_{low} is somewhere between F_{low}^{-} and F_{high}. In this case, the steady state, the concentrations of free MUNC18 and free tSNARE are virtually zero, which mean all of these proteins exist in the forms of FHC and FHC**.

(*ii*) Otherwise, there exists only one steady state that is locally stable, and the final fusion F is somewhere between $(0,F_{high})$.

Hence, with the regulation of MUNC18, the steady states of final level of fusion is controlled by the initial concentration of MUNC18: The behavior of bi-stability exists only when the initial concentration of MUNC18 is intermediate, whereas the boundary is determined by initial concentrations of tSNARE, VAMP2 and FHC. A lower or higher $[MUNC18]_0$ results in a single steady state of the final fusion level. Moreover, the final fusion level depends on $[tSNARE]_0$, suggesting that the preincubation (preform) of tSNARE is an important factor. Indeed, using numerical simulations, we have shown that for the system involving SNARE proteins, complexes and MUNC18, preformed assays have two advantages over the sequential one: first, preincubation advances reaction rates; second, preincubation support more fusion than sequential assays. Finally, we comment that the regulation mechanism of MUNC18 may be threshold dependent, i.e. there exists an optimal threshold ? which depends on the initial concentration of tSNARE and four helical bundle only, such that MUNC18's regulation function during fusion is maximized when the initial concentration of MUNC18 reaches the threshold (Xia et al, unpublished results).

Conclusive Remarks

In this study, we present a framework for modeling protein interaction network which are involved exocytotic process. The framework is based on classic chemical kinetic model that generates insights into system dynamics and stability. The computational experiments and mathematical analysis reveal that the frame reconstruct biological experimental observation successfully and is able to provide useful predictions.

Methods

Simulation Procedures

The kinetics simulation and analysis of the whole system or the subsystems were implemented in Matlab7.0R. Differential equations were solved using the ODE23s routine. For testing the robustness of parameters, we generated 2000 random parameter sets using Latin Hypercube Sampling when all parameters are varied $\pm 30\%$ relative to their original values, with a a uniform distribution for each parameter.

The concentrations of reactant proteins are given in molar units. For non-soluble proteins such as vSNARE and VAMP2, we followed the work in [10] and based the protein concentration estimation on the concentration of secretory vesicles in molar. During the exocytotic process, the size of vesicle pools varies with respect to different cell types from 200 to 3000. Hence, the molar concentration of vesicles was estimated in the range of 0.2–30 *nm*. Accordingly, the concentration of VAMP2 is considered to be in an identical range of vesicle concentration (0.2–30 *nm*) [10]. The tSNARE proteins such as SNAP25 and syntaxin are thought to be vastly expressed in vivo and the studies [1–6] evaluated the concentration of these protein in a range of 0.1–100 μm. The essential regulatory protein Munc18 is known to be expressed at much lower levels, compared to SNARE proteins, with the concentrations in range of 1–30 *nm* [3–4,10].

Algorithm for the Estimation of Rate Parameters

To recover the appropriate reaction rates, we apply technique of solving the inverse problem introduced by [27] to Eq.(10). Some useful results are presented below. To be concise, the ODE system Eq.(10) is written as $A(p)U=0$, U_0 is the initial conditions, and the parameter set $p=(k_{\pm 1},k_{\pm 2},c)$.

The inverse problem claims that the parameter identification of Eq.(10) is equivalent to the optimization problem of.

$$p_\alpha = arg \min_{U\in C[0,T),p\in\mathcal{P}} J(p) \tag{14}$$

subject to $A(p)U=0$ and $U(0)=U_0$, where $\mathcal{P}$ is the parameter space in R_+^5 and $J(p)$ is regularized energy functional

$$J(p)=\frac{M}{2}||QU_p-U_e||^2+\alpha||p||^2+e^{||-p||^2} \tag{15}$$

where M and α are Tikhonov regularization parameter [25], Q is parameter-data mapping, U_e is experimental data, and $e^{||-p||^2}$ is the penalty function to guarantee the positivity of reaction rates.

The rational of the inverse problem is based on the following theorem: Suppose the solution of Eq.(10) $U=(u_1,u_2,u_3,v_1,x)$ is smooth, where $[0,T)$ is the observation time. Then, given observed data on each time point in $[0,T)$, the parameters identified by the inverse problem are locally unique with respect to the initial condition. Under the assumption that all of the reaction rates are roughly constant, the optimization problem is solved through a gradient-based method. The brief algorithm is sketched below:

1. Given initial condition U_0, solving ODE system (3.1) by fourth order RK and mapping it on the observation data set,
2. Gradient representation: using forward difference to approximate ∇J,
3. Applying steepest descent to approach the global minimum starting with some initial guess,
4. Using adjoint scheme to approximate Hessian $\nabla^2 J$ of J,
5. Using the approximate solution given by step 2 as initial guess , and using Quasi-Newton method with $\nabla^2 J$ to find the appropriate parameter.

Stabilizing Analysis of the Fundamental Subsystem

The formal claim from the stabilizing analysis of the fundamental subsystem Eq.(10) is as follows: Define $c_2=u_3(0)+v_2(0)$, and $c_3=u_1(0)+v_1(0)+v_2(0)$ and $K=k_{-1}/k_1$. Let $\bar{u}_i$ $(i=1,2,3)$ and $\bar{v}_i$ $(i=1,2)$ be the steady-states for $[SNAP25]$, $[syntaxin]$, $[VAMP2]$, $[tSNARE]$, and $[FHC]$, respectively, and the steady-state vector $P=(\bar{u}_1,\bar{u}_2,\bar{u}_3,\bar{v}_1,\bar{v}_2)$.

Case-*A*. Assume the initial concentrations of SNAP25 and syntaxin are the same so that $c_1=0$. Denote $K=k_{-1}/k_1$, provided $k_{-2}<<k_2$. There are two stable steady states, P_1 and P_2: (*i*) If $c_2>c_3$, we have.

$$P_1=(0,0,c_2-c_3,0,c_3); \tag{16}$$

and (*ii*) otherwise

$$P_2=\left(\frac{1}{2}\left[-K+\sqrt{K^2-4K(c_2-c_3)}\right],\right.$$
$$\frac{1}{2}\left[-K+\sqrt{K^2-4K(c_2-c_3)}\right],$$
$$\left.0,c_3-c_2-\frac{1}{2}\left[-K+\sqrt{K^2-4K(c_2-c_3)}\right],c_2\right)$$

If $c_2=c_3$, the reduced steady state is $P=(0,0,0,0,c_3)$, which is locally stable.

Case-*B*. Consider the case of $c_1\neq 0$. Provided $k_{-i}<<k_i$ where $i=1,2$, there are four steady states:

(*i*) if $c_1\leq 0$ and $c_3\geq c_2$, the steady state is $P_1=(0,-c_1,0,c_3-c_2,c_2)$ and it is stable locally;

(*ii*) if $c_1\leq 0$ and $c_3\leq c_2$, the steady state is $P_2=(0,-c_1,c_2-c_3,0,c_3)$ and it is a stable node locally;

(*iii*) if $c_1\geq 0$ and $c_3\geq c_2+c_1$, the steady state is $P_3=(c_1,0,0,c_3-c_2-c_1,c_2)$ and it is stable locally;

(*iv*) if $c_1\geq 0$, $c_3\leq c_2+c_1$, and $c_3\geq c_1$, the steady state is $P_4=(c_1,0,c_2+c_1-c_3,0,c_3-c_1)$ and it is a stable node locally.

Case-C. A more general case is that the reaction ratios ($K:=k_{-1}/k_1$, $K'=k_{-2}/k_2$) and concentrations of SNARE proteins and complexes are in the same order, i.e., $K\in(10^{-8}M,10^{-6}M)$ and $K'\sim 10^{-10}M$. The steady states are.

$$P_1=(0,-c_1,c_2-c_3,0,c_3),\ \textit{if}\ \ c_1\leq 0\ \textit{and}\ c_3\leq c_2$$

$$P_2=(c_1,0,c_2+c_1-c_3,0,c_3-c_1),\ \text{if}\ \ c_1\geq 0,\ c_3\leq c_2+c_1,$$

$$\text{and}\ \ c_3\geq c_1 \tag{18}$$

and if $c_3\geq c_2$ and $c_3\geq c_2+c_1$

$$P_3=(u^*,u^*-c_1,0,c_3-u^*-c_2,c_2) \tag{19}$$

where

$$u^*=\frac{1}{2}[(c_1-K)\pm\sqrt{(K-c_1)^2-4K(c_2-c_3)}]. \tag{20}$$

Note that P_1,P_2 and P_3 are locally stable nodes. When K is small sufficiently comparing to the concentrations of SNARE proteins and complexes, P_3 is reduced to.

$$P_{3'}=(0,-c_1,0,c_3-c_2,c_2)$$

$$P_{3''}=(c_1,0,0,c_3-c_2-c_1,c_2). \tag{21}$$

Proof. A concise proof is presented below. From the definition of c_1 to c_3, straightforward calculation simplifies the fundamental subsystem Eq.(10) as follows.

$$\frac{du_1}{dt}=k_1u_1(u_1-c_1)+k_{-1}(c_3-u_1-v_2)$$

$$\frac{dv_2}{dt}=k_2(c_3-u_1-v_2)(c_2-v_2)-k_{-2}v_2 \tag{22}$$

For Case-A that $c_1=0$, Eq.(22) can be further simplified to be.

$$\frac{du_1}{dt}=k_1u_1^2+k_{-1}(c_3-u_1-v_2)$$

$$\frac{dv_2}{dt}=k_2(c_3-u_1-v_2)(c_2-v_2)-k_{-2}v_2 \tag{23}$$

Notice that reaction rates recovered from the experimental data imply $k_{-2}/k_2\sim 10^{-10}M$, so that compared to the concentrations of SNARE complexes, k_{-2}/k_2 is negligible. Thus, the v_2-nullcline determined by Eq.(23) so that.

$$n_{v_2}=\{v_2:(c_3-u_1-v_2)(c_2-v_2)=0\}$$

Denote $K=k_{-1}/k_1$, u_1-nullcline is given by.

$$n_{u_1}=\{u_1:u_1=\frac{1}{2}[-K\pm\sqrt{K^2-4K(v_2-c_3)}\}$$

The steady states are yielded by intersecting the nullclines, and the biological interesting steady states are therefore given by P_1 and P_2. Straightforward calculation implies the steady states P_1 and P_2 are a pair of opposite vertexes, and the relationship of c_3 and c_2 determines the choice of these two steady states. If $c_2>c_3$, the only possible steady state is P_1; if $c_2<c_3$, the only possible steady state is P_2.

To investigate the stability of those steady states, we calculated the corresponding Jacobian for system Eq.(23) and then evaluate the two eigenvalues, denoted by λ_1 and λ_2, respectively. For steady state P_2, two eigenvalues for the Jacobian have no zero real part because of $c_2<c_3$, so that steady state P_2 is a hyperbolic point of system Eq.(23). By Hartman-Grobman theorem, there exists a homeomorphism mapping the trajectories of Eq.(23) in an open set containing P_2 onto trajectories of its linearized system in an open set containing P_2. Furthermore, the homeomorphism preserves the parameterizations by time. Therefore, local behaviors of P_2 is characterized by its corresponding Jacobian, leading to $\lambda_1<0$ and $\lambda_2<2$. Therefore, steady state P_2 is stable locally.

For steady state P_1, we calculated the corresponding Jacobian and showed that none of the eigenvalues has zero real part, so that P_1 is a hyperbolic steady point of system Eq.(23). The local behavior of trajectories of (Eq.(23) in the neighborhood of P_1 is

characterized by its linearized system with respect to P_1. As the trace of correspondiong Jacobian is less than zero, we show P_1 is stable locally.

In the same manner, we have shown the results presented in case-B and case-C.

Stabilizing Analysis of MUNC-18 Regulation

For the system described in Eq.(17), there are three steady states, which are.if $v_1(0) \le u_3(0)+u_4(0_+ v_3(0)$ and thus $v_2(0)+v_1(0) \ge u_4(0)$,then

$$P=(u_3,u_4,v_1,v_2,v_3)=(0,0,x-c_2,c_1-x,x) \tag{24}$$

for any $x \in [c_2,c_1]$, or

$$P=(u_3,u_4,v_1,v_2,v_3)=(c_2-x,0,0,c_1-c_2,x) \tag{25}$$

for any $x \in [0,c_2]$.if $v_2(0)+v_1(0) \le u_4(0)$, then

$$P=(u_3,u_4,v_1,v_2,v_3)=(c_1-x,c_2-c_1,0,0,x) \tag{26}$$

for any $x \in [0,c_1]$.where $c_1=v_2(0)+v_3(0)+u_3(0)$ and $c_2=u_3(0)-v_1(0)+u_4(0)+v_3(0)$. These steady states are locally stable.

Proof: The proof is similar to the case of system Eq.(10) without regulation.

Acknowledgments

We would like to thank Yeon-Kyun Shin, Jian-Song Tong, and Julia Dickerson for their valuable suggestions and comments.

Author Contributions

Carried out the study: WC WZ TX XG. Coordinated the project and the manuscript preparation: XG. Carried out the mathematical analysis and drafted the manuscript: WC WZ. Carried out the data and simulation analyses: TX. Read and approved the final manuscript: WC WZ TX XG.

References

1. Weber T, Zemelman BV, McNew JA, Westermann B, Gmachl M, et al. (1998) SNAREpins: Minimal Machinery for Membrane Fusion. Cell 92: 759–772.
2. Sollner T, Bennett MK, Whiteheart SW, Scheller R, Rothman JA (1993) Protein assembly-disassembly pathway in vitro that may correspond to sequential steps of synaptic vesicle docking, activatgion, and fusion. Cell 75: 409–418.
3. Chen YA, Scheller RH (2001) SNARE-mediated membrane fusion. Nat Rev Mol Cell Biol 2: 98–106.
4. Burgoyne RD, A. Morgan A (2003) Secretary Granule Exocytosis. Physiol Rev 83: 581–632.
5. Lin RC, Scheller RH (2000) Mechanisms of synaptic vesicle exocytosis. Annu Rev Cell Dev Biol 16: 19–49.
6. Burgoyne RD, Morgan A (2007) Membrane trafficking: three steps to fusion. Curr Biol 17: 255–258.
7. Heinemann C, Ruden LV, Chow RH, Neher E (1993) A two-step model of secretion control in neuroendocrine cells. Pflügers Arch, 424: 105–112.
8. Jahn R, Lang T, Sudhof TC (2003) Membrane fusion. Cell, 112: 519–533.
9. Lu XB, Zhang F, McNew JA, Shin YK (2005) Membrane fusion induced by neuronal SNAREs transits through hemifusion. J Biol Chem 280: 30538–30541.
10. Mezer A, Nachliel E, Gutman M, Ashery U (2004) A new platform to study the molecular mechanisms of exocytosis. J Neurosci 24: 8838–8846.
11. Moser T, Neher E (1997), "Estimation of mean exocytic vesicle capacitance in mouse adrenal chromaffin cells," Proc Natl Acad Sci USA 94: 6735–6740.
12. Misura KMS, Schelle RH, Weis WI (2001) Self-association of the h3 region of syntaxin 1a implications for intermediates in snare complex assembly. J Biol Chem 276: 13273–13282.
13. Sudhof TC (2004) The synaptic vesicle cycle. Annu Rev Neurosci 27: 509–547.
14. Brose N, Petrenko AG, Sudhof TC, Jahn R (1992) Synaptotagmin: a calcium sensor on the synaptic vesicle surface. Science 256: 1021–1025.
15. Chapman ER (2002) Synaptotagmin: a Ca^{2+} sensor that triggers exocytosis? Nat Rev Mol Cell Biol 3: 498–508.
16. Bhalla A, Chicka MC, Tucker WC, Chapman ER (2006) Ca^{2+} -synaptotagmin directly regulates t-SNARE function during reconstituted membrane fusion. Nature Struc Mol Biol 13: 323–330.
17. Ciufo LF, Barclay JW, Burgoyne RD, Morgan A (2005) Munc18–1 regulates early and late stages of exocytosis via syntaxin-independent protein interactions. Mol Biol Cell 16: 470–482.
18. Margittai M, Widengren J, Schweinberger E, Schroder GF, Felekyan S, et al. (2003) Single-molecule fluroscence resonance energy transfer reveals a dynamic equilibrium between closed an dopen conformations of syntaxin I. Proc Natl Acad Sci USA 100: 15516–15521.
19. Fasshauer D, Margittai M (2004) A transient N-terminal interaction of SNAP-25 and syntaxin nucleates SNARE assembly. J Biol Chem 279: 7613–7621.
20. Giraudo CG, Eng WS, Melia TJ, Rothman JE (2006) A clamping mechanism involved in SNARE-dependent exocytosis. Science, 313: 676–80.
21. Pobbati AV, Stein A, Fasshauer D (2006) N- to C-terminal SNARE complex assembly promotes rapid membrane fusion. Science 313: 673–676.
22. Shen JS, Tareste DC, Paumet F, Rothman JE, Melia TJ (2007) Selective activation of cognate SNAREpins by SEC1/MUNC18 proteins. Cell 128: 183–195.
23. Weninger K, Bowen ME, Chu S, Brunger AT (2003) Singel-molecule studies of SNARE complex assembly reveal parallel and antiparallel configurations. Proc Natl Acad Sci USA 100: 14800–14805.
24. Keener J, Sneyd J (2001) Mathematical Physiology, New York Springer-Verlag.
25. Lorenzi A (2001) An introduction to identification problems via functional analysis, Utrecht: VSP-BV.
26. Perko L (2000) Differential equations and dynamical systems, New YorkL Springer-Verlag.
27. Vogel CR (2002) Computational Methods for inverse problem, SIAM, 2002.
28. de Vries G, Hillen T, Lewis M, Muller J, Schonfisch B (2006) A course in mathematical biology-quantitative modeling with mathematical and computational methods, SIAM Philadelphia.
29. Xia T, Tong J, Rathore SS; Gu, X, Dickerson J (2012) Comparative network motif design rationalizes Sec1/Munc18-SNARE regulation mechanism in exocytosis. BMC Systems Biology (in press).